Atmospheric
Chemistry
and Physics
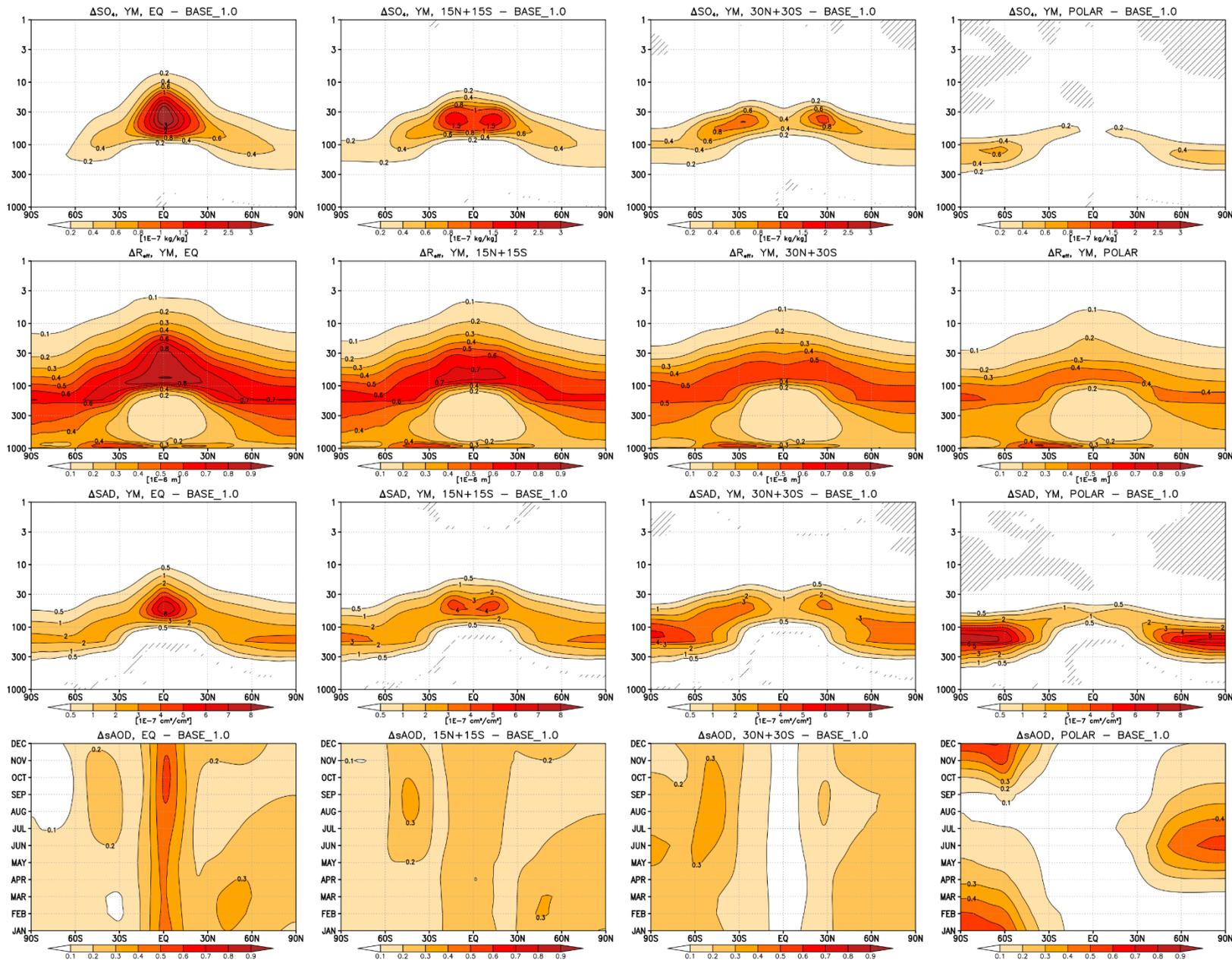
Supplement of

Injection strategy – a driver of atmospheric circulation and ozone response to stratospheric aerosol geoengineering

Ewa M. Bednarz et al.

*Correspondence to:* Ewa M. Bednarz (ewa.bednarz@noaa.gov)

Figure S1. (Top) Yearly mean changes in sulfate mass mixing ratios, (row 2) yearly mean aerosol effective radius, (row 3) yearly mean changes in sulfate surface area density, and (bottom) spatiotemporal evolution of simulated AOD changes in EQ, 15N+15S, 30N+30S and POLAR strategy compared, if applicable, to the baseline period (2008-2027). Hatching in rows 1, 3, 4 indicate regions where the response is not statistically significant, taken as smaller than ±2 standard errors of the difference in means.
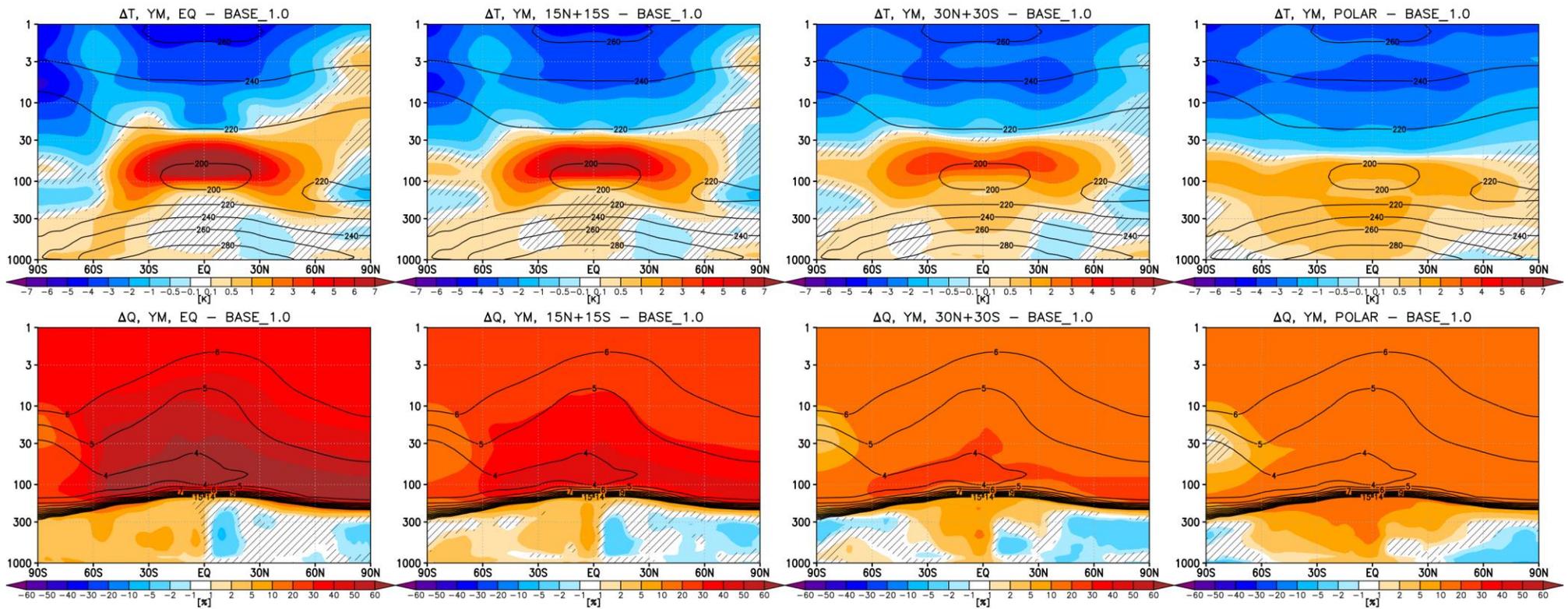
Figure S2. Shading: yearly mean changes in (top) temperatures and (bottom) water vapour for (left to right) EQ, 15N+15S, 30N+30S and POLAR strategy compared to the baseline period (2008-2027). Contours show the corresponding values in the baseline period for refence (in units of K and ppm for temperature and water vapour respectively). Hatching indicates regions where the response is not statistically significant, taken as smaller than ±2 standard errors of the difference in means.
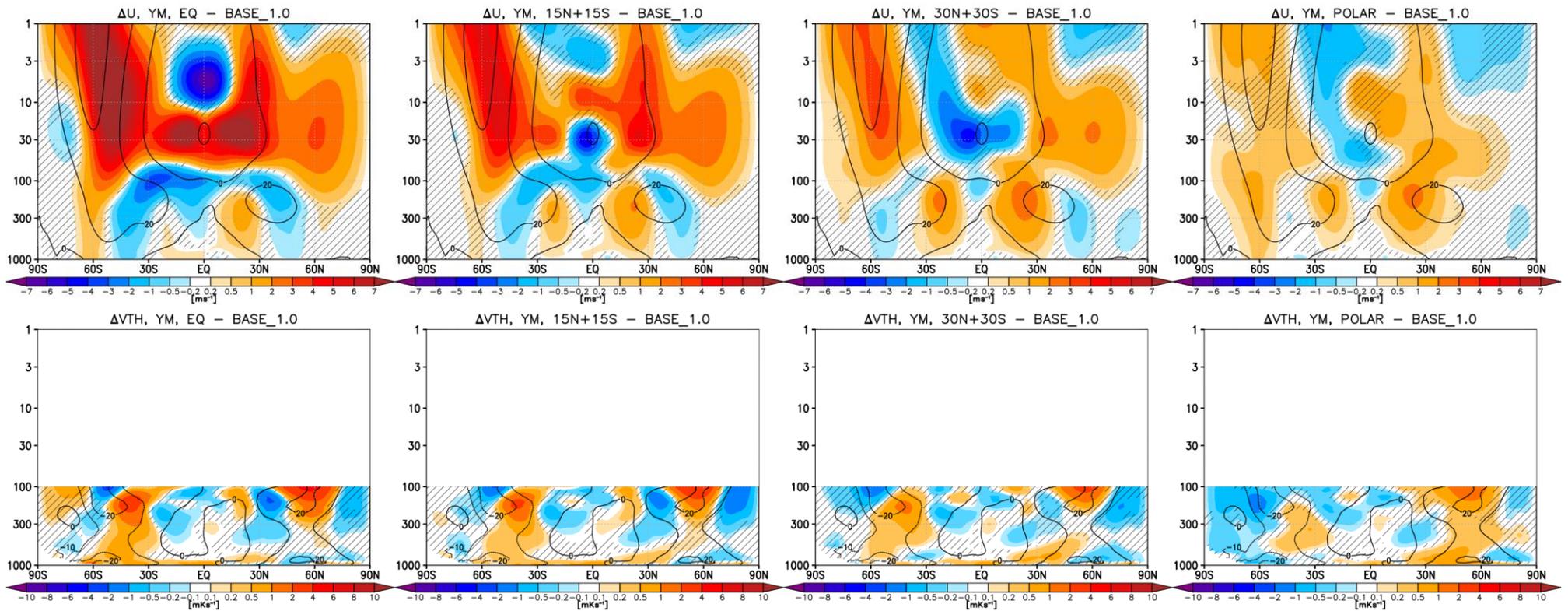
Figure S3. Shading: yearly mean changes in (top) zonal winds and (bottom) northward meridional eddy heat flux for (left to right) EQ, 15N+15S, 30N+30S and POLAR strategy compared to the baseline period (2008-2027). Contours show the corresponding values in the baseline period for refence. Hatching as in Fig. S2.

4
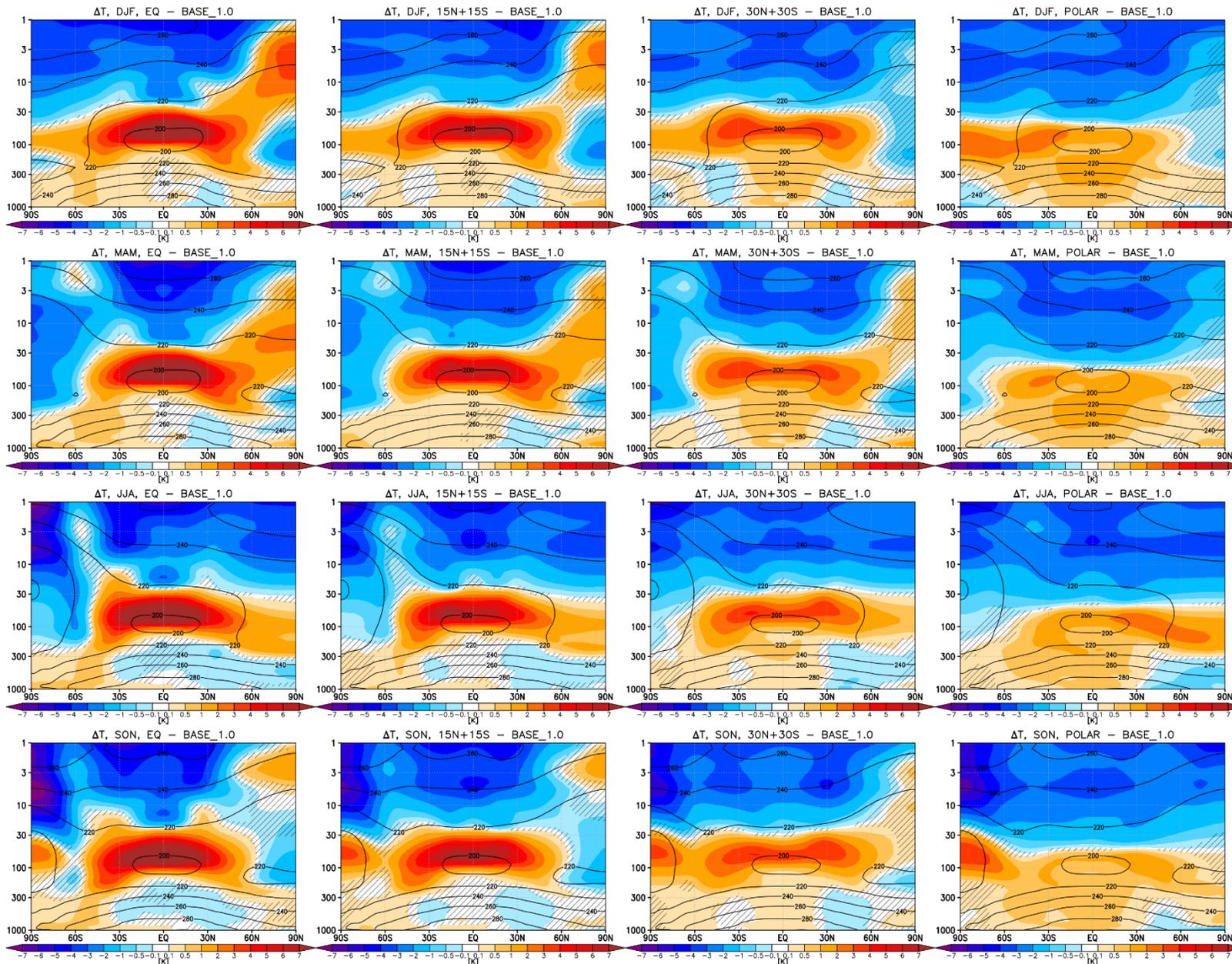
Figure S4. Shading: Seasonal mean (top to bottom: DJF, MAM, JJA and SON) changes in temperature [K] for (left to right) EQ, 15N+15S, 30N+30S and POLAR strategy compared to the baseline period (2008-2027). Contours show the corresponding values in the baseline period for refence. Hatching as in Fig. S2.
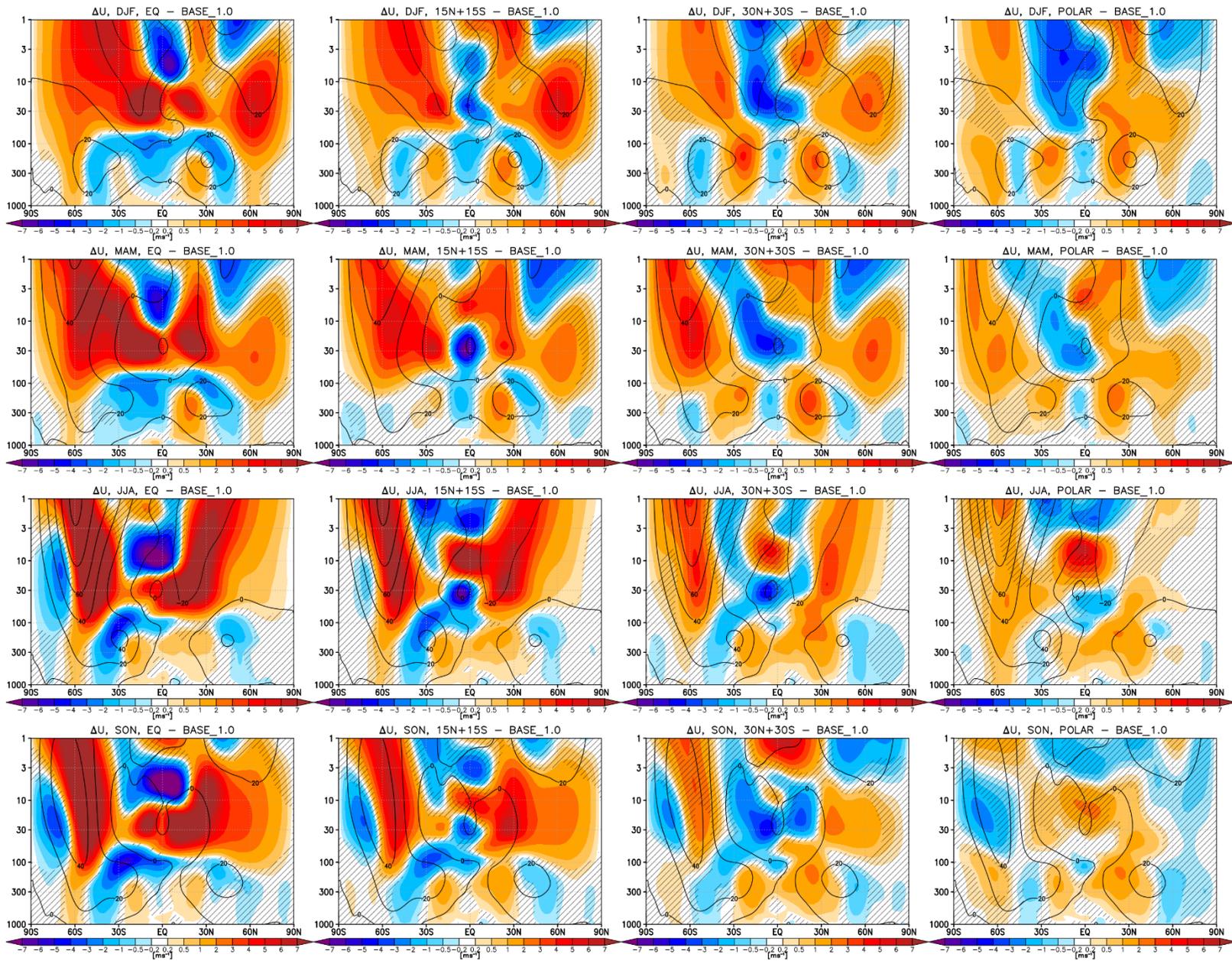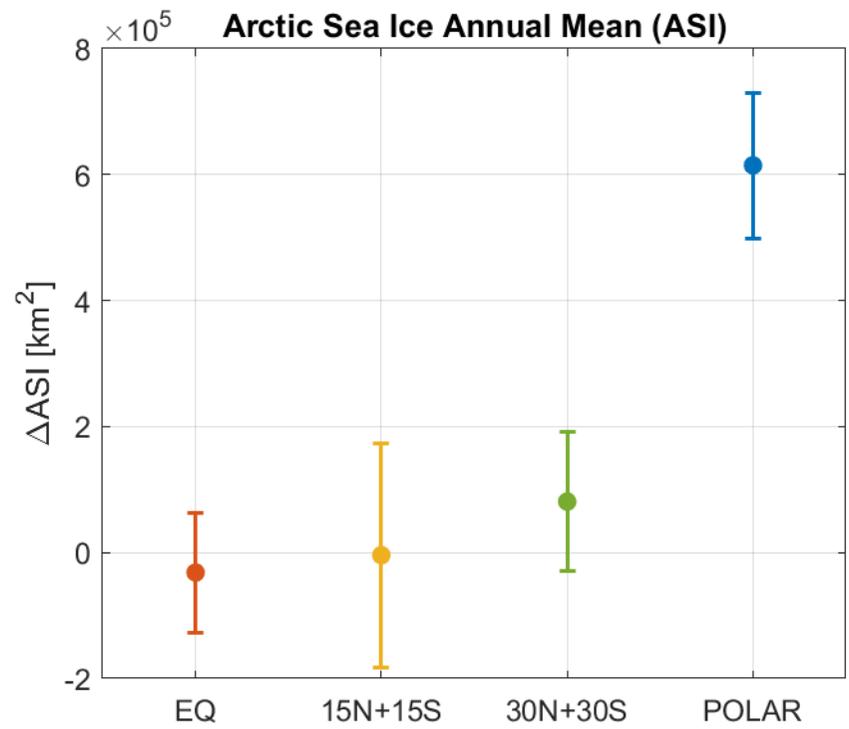
Figure S5. As in Fig. S4 but for the zonal winds [m/s].

Figure S6. Yearly mean changes in the Arctic sea-ice extent for each of the injection strategy compared to the baseline period. The errorbars denote ±2 standard errors of the mean of each SAI strategy.
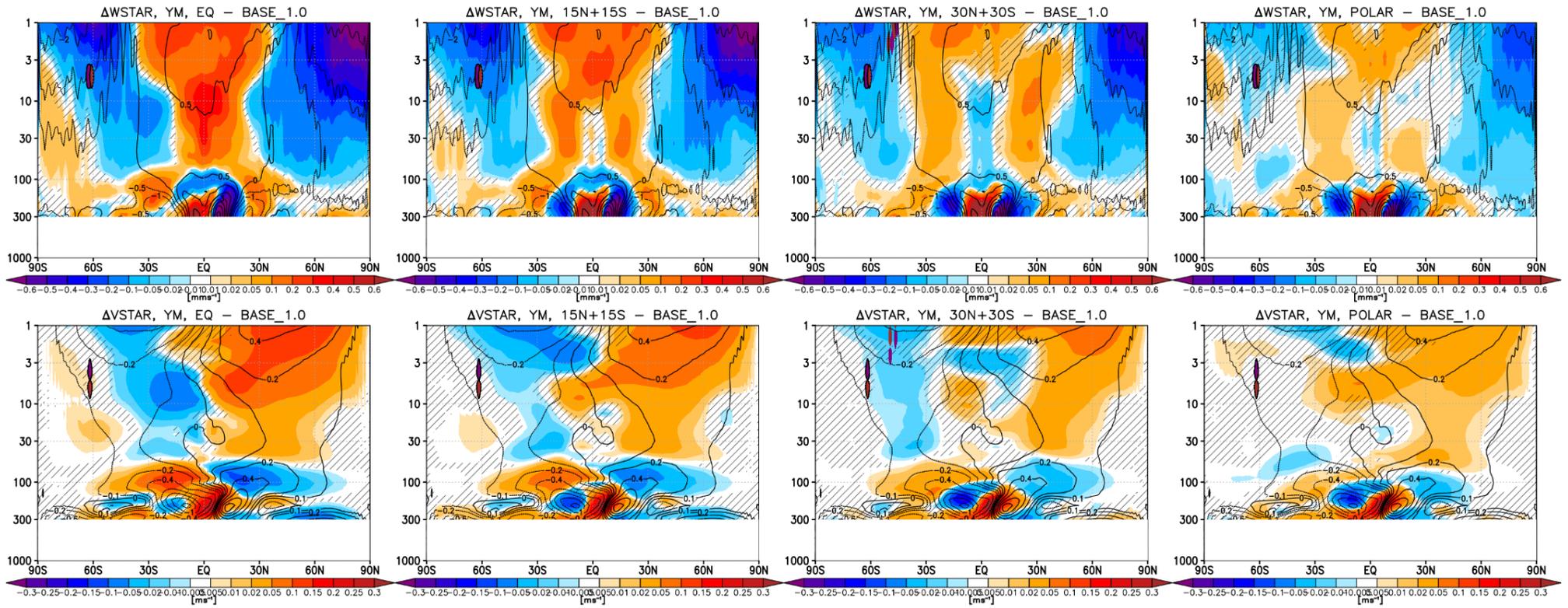
Figure S7. As in Fig. S2 but for the changes in TEM (top) vertical and (bottom) meridional velocities. Hatching as in Fig. S2.
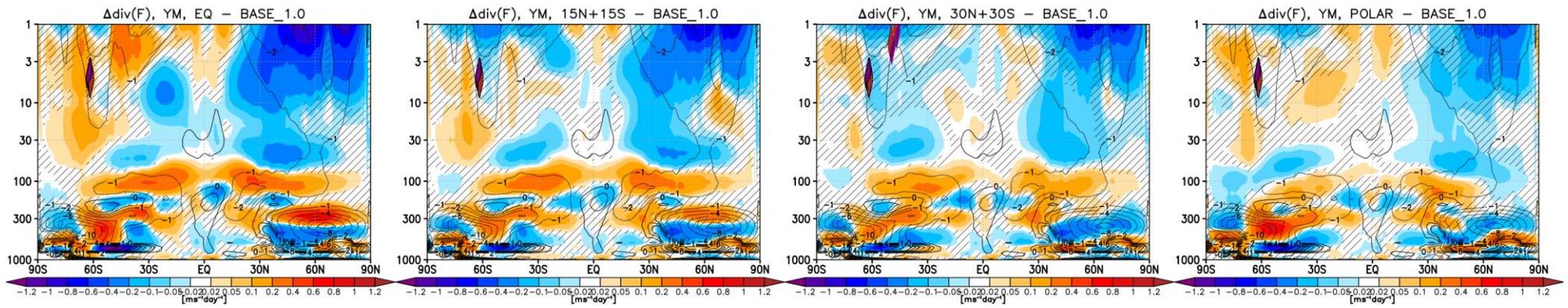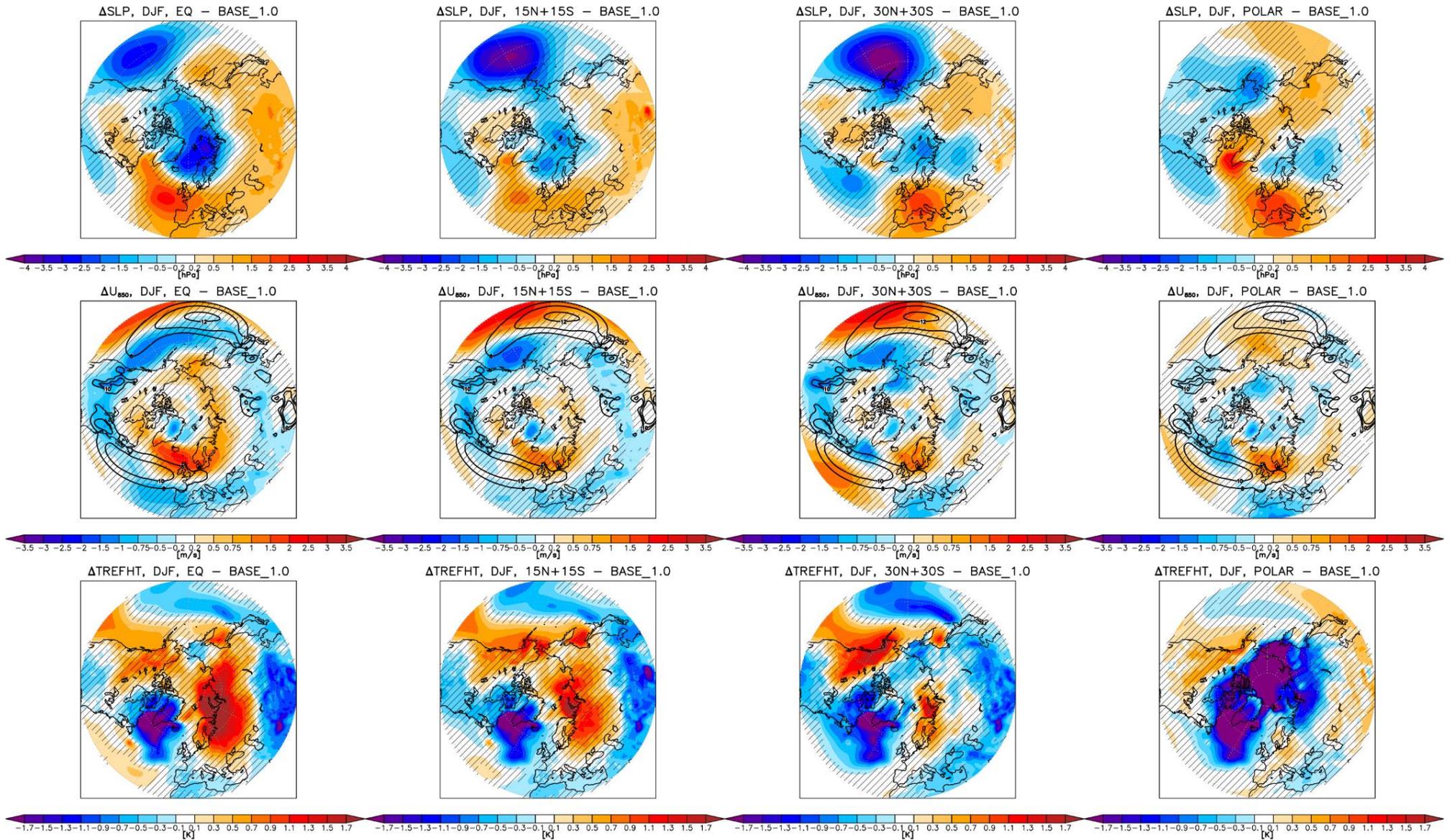
Figure S8. As in Fig. S2 but for the changes in the EP flux divergence. Hatching as in Fig. S2.
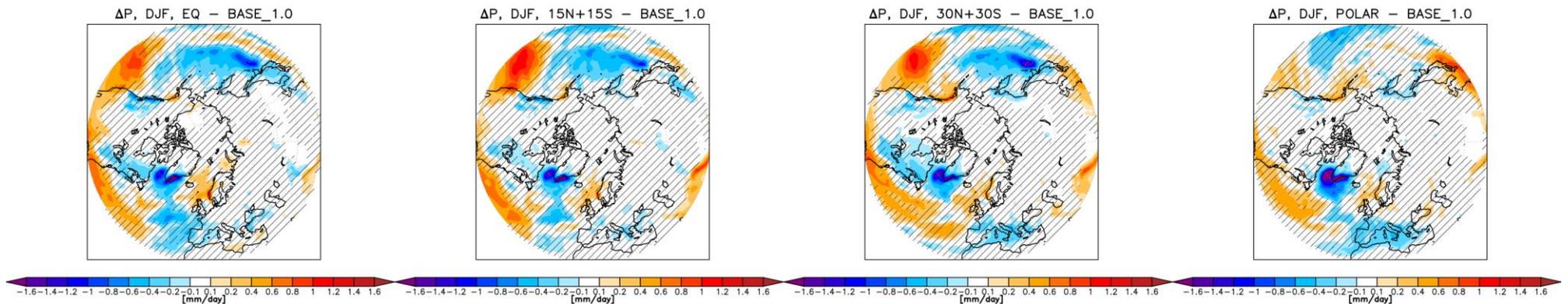
Figure S9. Shading: DJF mean changes in (top) sea-level pressure, (middle) zonal wind at 850 hPa and (bottom) near-surface atmospheric temperatures northward from 30°N for (left to right) EQ, 15N+15S, 30N+30S and POLAR strategy compared to the baseline period (2008-2027).
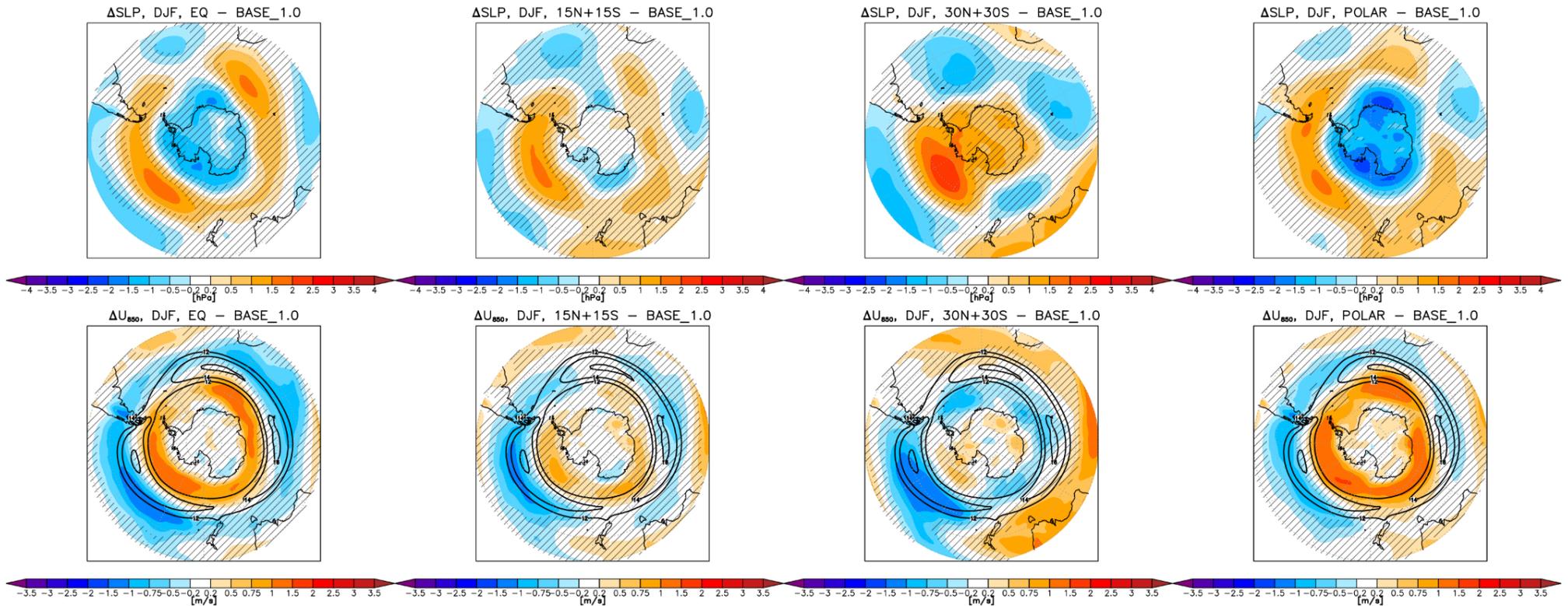
Contours in (middle) show the corresponding values in the baseline period for refence and denote the position of the climatological jet. Hatching as in Fig. S2.
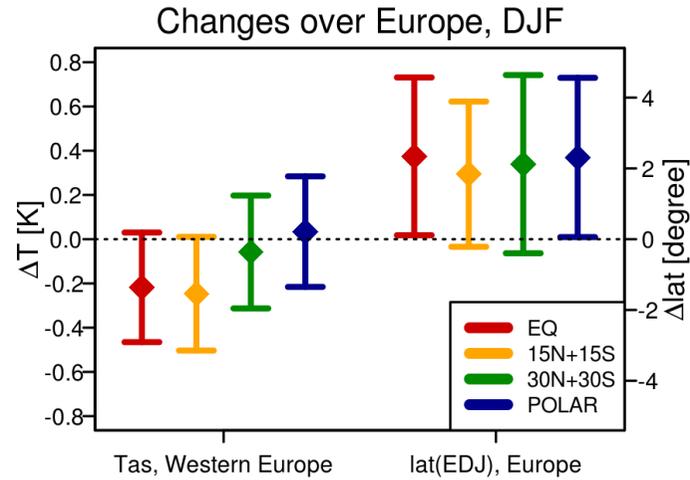

Figure S10. DJF mean changes in (left) near-surface atmospheric temperature over the western Europe (defined as the area spanning 10°W-10°E, 30°N-50°N) and (right) position of the NH eddy-driven jet over Europe (defined as 10°W-30°E) for each of the four strategies compared to the baseline period. The errorbars denote ±2 standard error of the difference in means.
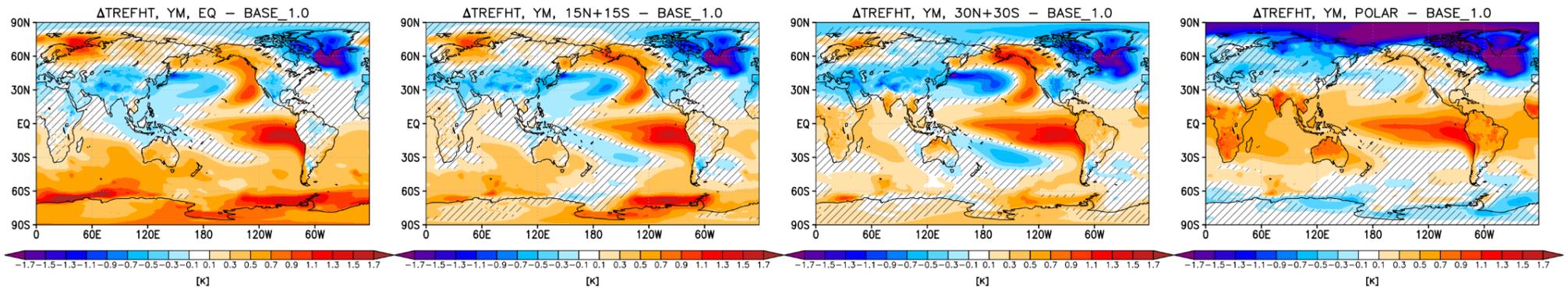

Figure S11. DJF mean changes in total precipitation northward from 30°N for (left to right) EQ, 15N+15S, 30N+30S and POLAR strategy compared to the baseline period (2008-2027). Hatching as in Fig. S2.

11

Figure S12. Shading: DJF mean changes in (top) sea-level pressure, and (bottom) zonal wind at 850 hPa southward from 30°S for (left to right) EQ, 15N+15S, 30N+30S and POLAR strategy compared to the baseline period (2008-2027). Contours in (bottom) show the corresponding values in the baseline period for refence and denote the position of the climatological jet. Hatching as in Fig. S2.
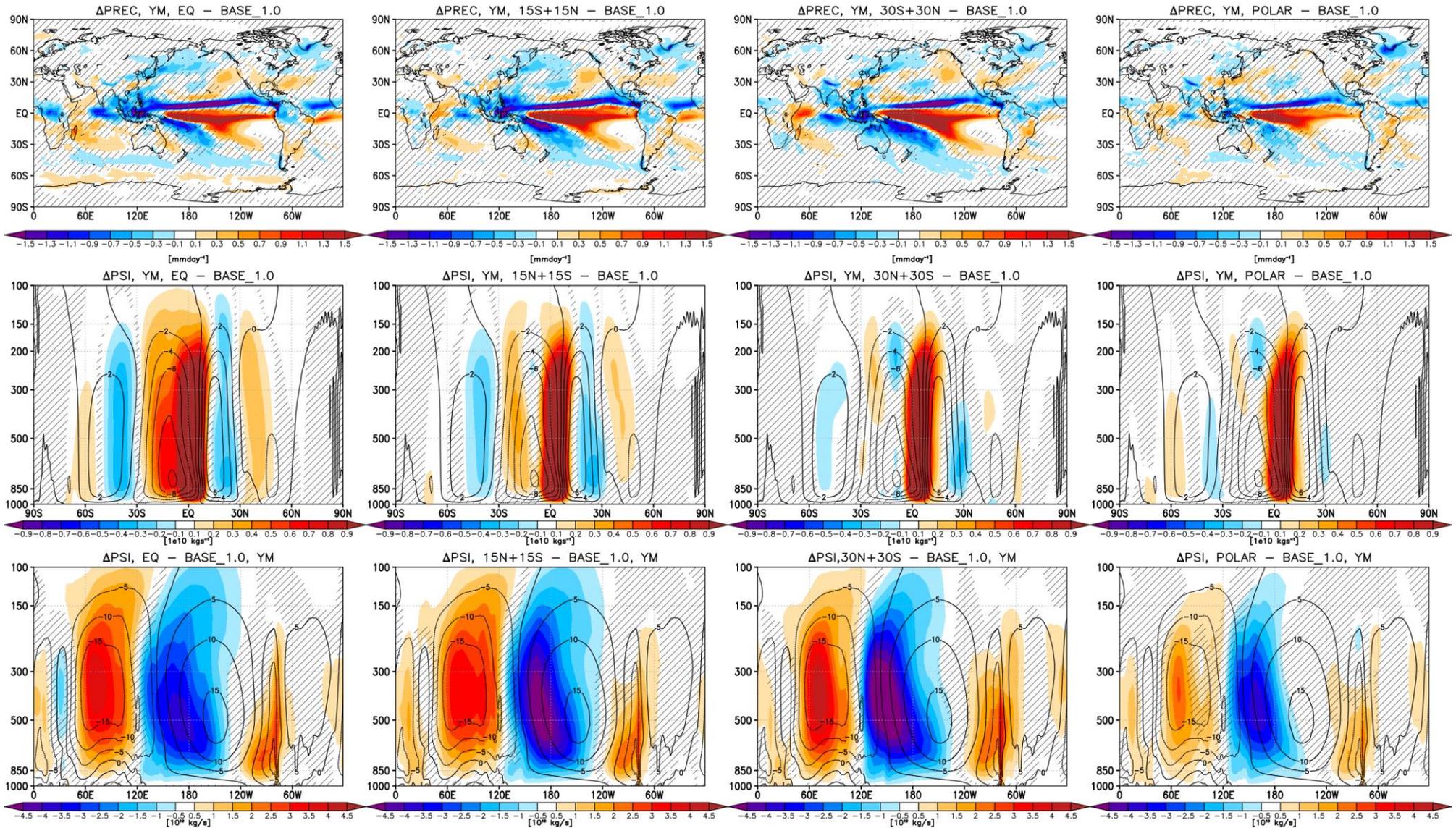
Figure S13. Shading: Yearly mean changes in (top) precipitation, (middle) meridional mass stream function, and (bottom) zonal mass stream function for (left to right) EQ, 15N+15S, 30N+30S and POLAR strategy compared to the baseline period (2008-2027). Contours show the corresponding values in the baseline period for refence. Hatching as in Fig. S2.

Figure S14. Yearly mean changes in near-surface air temperatures for (left to right) EQ, 15N+15S, 30N+30S and POLAR strategy compared to the baseline period. Hatching as in Fig. S2.
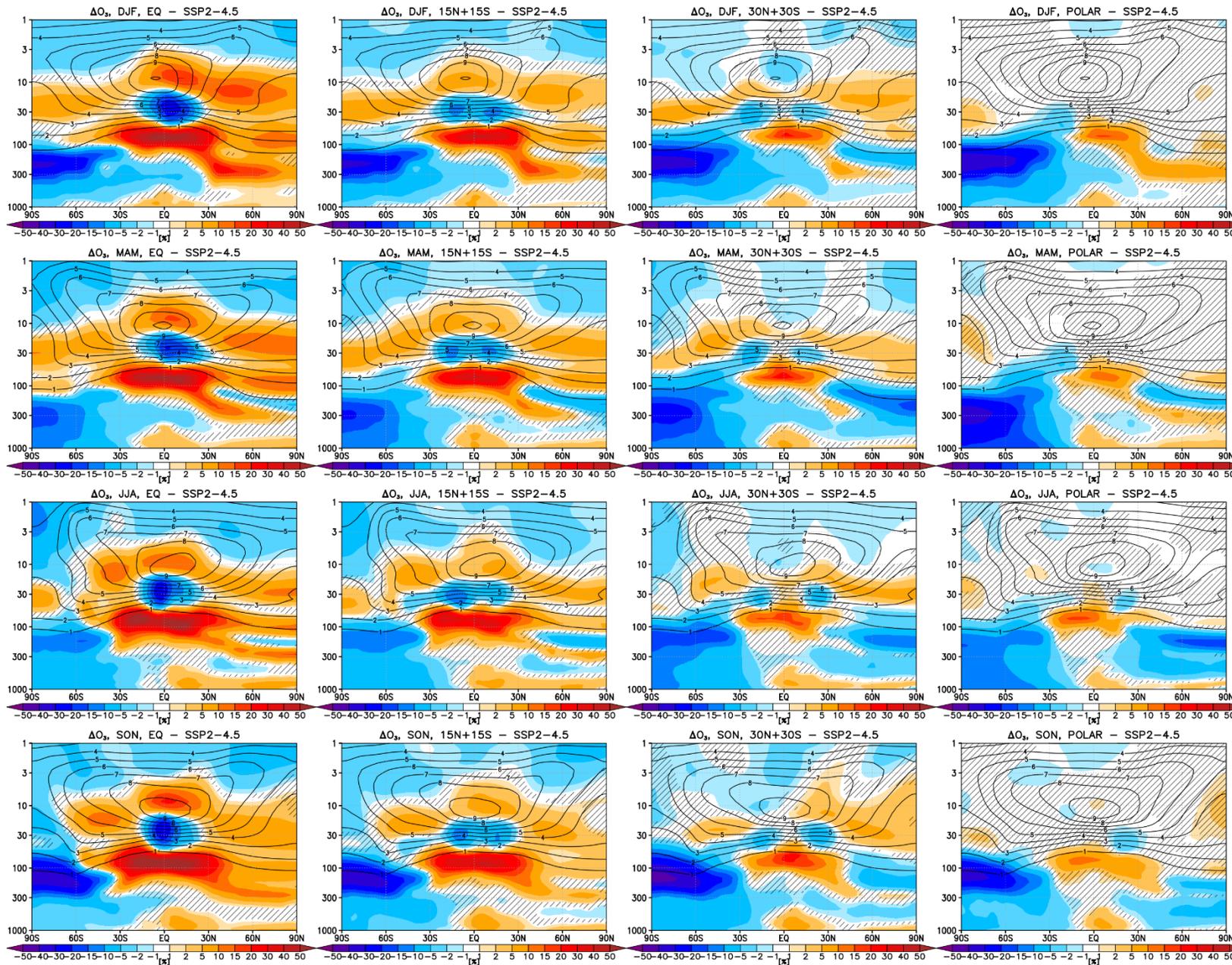
Figure S15. Shading: Seasonal mean (top to bottom: DJF, MAM, JJA and SON) changes in ozone mixing ratios (left to right) EQ, 15N+15S, 30N+30S and POLAR strategy compared to the same period (i.e. 2050-2069) of the control SSP2-4.5 simulation. Contours show the corresponding values in SSP2-4.5 for refence (in the units of ppm). Hatching as in Fig. S2.

Figure S16. Yearly mean changes in (top) NO$_x$ [ppb], (middle) ClO$_x$ [ppt] and (bottom) BrO$_x$ [ppt] simulated in each of the SAI strategy (columns) compared to the same period of the SSP2-4.5 simulation. Contours show the values in the corresponding values in SSP2-4.5 for reference. Hatching as in Fig. S2.